

# Robust Spin Fluctuations and $s\pm$ Pairing in the Heavily Electron Doped Iron-Based Superconductors

Katsuhiro Suzuki<sup>1</sup>, Hidetomo Usui<sup>2</sup>, Kazuhiko Kuroki<sup>2</sup>, Soshi Iimura<sup>3</sup>,  
Yoshiyasu Sato<sup>3</sup>, Satoru Matsuishi<sup>4</sup>, and Hideo Hosono<sup>5</sup>

<sup>1</sup> *Department of Engineering Science, The University of Electro-Communication, Chofu, Tokyo 182-8585, Japan*

<sup>2</sup> *Department of Physics, Osaka University, 1-1 Machikaneyama, Toyonaka, Osaka 560-0043, Japan*

<sup>3</sup> *Materials and Structures Laboratory, Tokyo Institute of Technology, 4259 Nagatsuta-cho, Midori-ku, Yokohama 226-8503, Japan*

<sup>4</sup> *Materials Research Center for Element Strategy, Tokyo Institute of Technology, 4259 Nagatsuta-cho, Midori-ku, Yokohama 226-8503, Japan*

<sup>5</sup> *Frontier Research Center, Tokyo Institute of Technology, 4259 Nagatsuta-cho, Midori-ku, Yokohama 226-8503, Japan*

We theoretically study the spin fluctuation and superconductivity in La1111 and Sm1111 iron-based superconductors for a wide range of electron doping. When we take into account the band structure variation by electron doping, the hole Fermi surface originating from the  $d_{X^2-Y^2}$  orbital turns out to be robust against electron doping, and this gives rise to large spin fluctuations and consequently  $s\pm$  pairing even in the heavily doped regime. The stable hole Fermi surface is larger for Sm1111 than for La1111, which can be considered as the origin of the apparent difference in the phase diagram.

KEYWORDS: iron pnictide superconductors, Fermi surface, spin fluctuation, first-principles band calculation

The pairing mechanism of the iron-based superconductors has been of great interest ever since its discovery.<sup>1)</sup> The possibility of spin-fluctuation-mediated pairing in the iron-based superconductors has been proposed from the very beginning of the study.<sup>2-4)</sup> The key point here is the presence of the disconnected electron and hole Fermi surfaces, which gives rise to spin fluctuations around the wave vector that connects the Fermi surfaces. The resulting pairing state is the so-called  $s\pm$  state in which the sign of the gap function changes between electron and hole Fermi surfaces.

Recent observation of superconductivity in “1111” compounds  $LnFeAsO_{1-x}H_x$  ( $Ln=La, Sm$ , etc.) for a wide range of  $x$ <sup>5,6)</sup> has raised an interesting issue regarding the possibility of spin-fluctuation-mediated pairing. There, the superconducting state persists up to a large  $x$  of  $\sim 0.4$ , for which hole Fermi surfaces are expected to be completely wiped out in a rigid band picture. In fact, theoretical studies based on the doping independent five orbital Hamiltonian show that the spin-fluctuation-mediated superconductivity is lost for about 20 percent ( $x=0.2$ ) electron doping,<sup>7-9)</sup> so that the observation of superconductivity in the heavily doped  $LnFeAsO_{1-x}H_x$  has led to a proposal of the pairing mechanism based on local orbital fluctuations,<sup>10)</sup> in which the Fermi surface nesting does not play an important role. Therefore, whether the spin fluctuation can be responsible for pairing even in such a heavily doped regime is certainly an intriguing problem.

To address this issue, in the present paper we study the spin fluctuations and superconductivity of La1111 and Sm1111 by applying random phase approximation (RPA) to a five orbital model that takes into account the effect of the variation of the band structure due to

electron doping. It is found that the hole Fermi surface around the wave vector  $(\pi, \pi)$  that originates from the  $d_{X^2-Y^2}$  orbital is robust against electron doping, and this induces large spin fluctuations and  $s\pm$  pairing even in the heavily electron doped regime. The stable hole Fermi surface is larger for Sm1111 than for La1111, and we propose that this is the origin of the difference in the experimentally observed  $T_c$  vs.  $x$  phase diagram, in which the latter material has a two-dome feature, while the former has a single-dome shape.<sup>5,6)</sup>

We start with the first principles band calculation for the two materials. The band calculation is performed using the VASP package<sup>11)</sup> for La1111 and Sm1111 compounds. Since the rigid band picture is expected to be unreliable especially in the heavily doped regime, we take into account the effect of the band structure variation due to doping by (i) adopting the lattice structure parameters determined experimentally for each doping rate  $x$ , and (ii) adopting virtual crystal approximation in which the oxygen and the fluorine pseudopotentials are mixed, assuming that the hydrogen doping has an effect of increasing the average valence of the oxygen site by  $+x$ .<sup>5)</sup> We construct a five orbital tight-binding Hamiltonian in the unfolded Brillouin zone<sup>3)</sup> exploiting the maximally localized Wannier functions.<sup>12)</sup> The five Wannier orbitals have five different symmetries ( $d_{XY}$ ,  $d_{YZ}$ ,  $d_{ZX}$ ,  $d_{3Z^2-R^2}$  and  $d_{X^2-Y^2}$ ), where  $X, Y$  refer to the direction rotated by 45 degrees from the Fe-Fe direction  $x, y$ .

We construct a many body Hamiltonian by taking into account the multi-orbital electron-electron interactions, and apply random phase approximation (RPA).<sup>13,14)</sup> Using the Green’s function  $G_{lm}(k)$  ( $k \equiv (\mathbf{k}, i\omega_n)$ ), which is a  $5 \times 5$  matrix in the orbital representation, the irre-

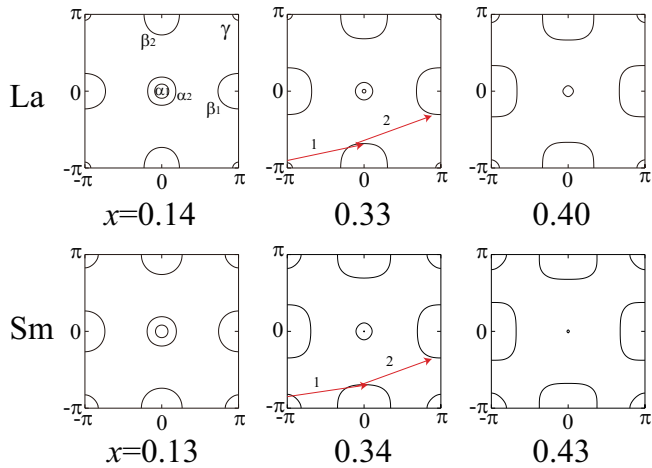


**Fig. 1.** (Color online) The Fermi surface for various doping rates for La1111 (top) and Sm1111 (bottom). The arrows 1 and 2 indicate the interactions between the Fermi surfaces which give rise to spin fluctuations and superconductivity.

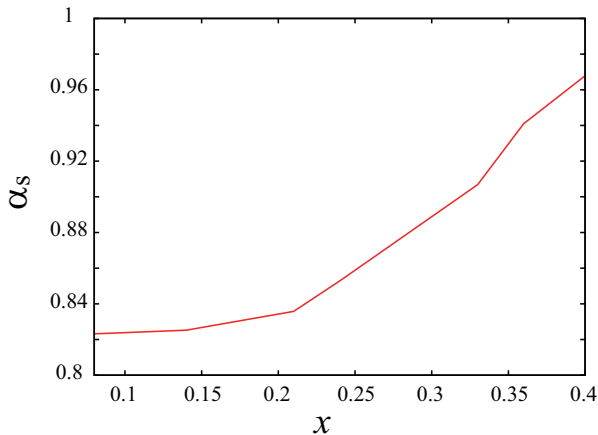


**Fig. 2.** (Color online) The Stoner factor for La1111 plotted against the doping rate.

ducible susceptibility matrix is given as

$$\chi_{l_1, l_2, l_3, l_4}^0(q) = \sum_k G_{l_1 l_3}(k+q) G_{l_4 l_2}(k), \quad (1)$$

and the spin and the charge (orbital) susceptibility matrices are obtained as

$$\hat{\chi}_s(q) = \frac{\hat{\chi}^0(q)}{1 - \hat{S}\hat{\chi}^0(q)}, \quad (2)$$

$$\hat{\chi}_c(q) = \frac{\hat{\chi}^0(q)}{1 + \hat{C}\hat{\chi}^0(q)}, \quad (3)$$

where  $\hat{S}$  and  $\hat{C}$  are the corresponding interacting vertex matrices. These matrices have  $l_1$  to  $l_4$  ( $l_i = 1, \dots, 5$ ) as orbital indices. We calculate the Stoner factor defined as the largest eigenvalue of the matrix  $\hat{S}\hat{\chi}^0(q)$ . This qualitatively measures the strength of the low energy spin fluctuations, and a tendency toward magnetism.

The Green's function and the effective singlet pairing

interaction,

$$\hat{V}^s(q) = \frac{3}{2}\hat{S}\hat{\chi}_s(q)\hat{S} - \frac{1}{2}\hat{C}\hat{\chi}_c(q)\hat{C} + \frac{1}{2}(\hat{S} + \hat{C}), \quad (4)$$

are plugged into the linearized Eliashberg equation for superconductivity,

$$\lambda\phi_{l_1 l_4}(k) = -\frac{T}{N} \sum_q \sum_{l_2 l_3 l_5 l_6} V_{l_1 l_2 l_3 l_4}(q) \times G_{l_2 l_5}(k-q)\phi_{l_5 l_6}(k-q)G_{l_3 l_6}(q-k) \quad (5)$$

The  $5 \times 5$  matrix gap function  $\phi_{lm}$  in the orbital representation along with the associated eigenvalue  $\lambda$  is obtained by solving this equation. Since  $\lambda(T) = 1$  signals  $T = T_c$ , the eigenvalue calculated at a fixed temperature is a qualitative measure for  $T_c$ . We present the gap function transformed into the band representation with a unitary transformation. The RPA calculation is performed for  $64 \times 64 \times 4$  sites and 2048 Matsubara frequencies, and the temperature is  $T = 0.02\text{eV}$ . The electron-electron interactions are taken from ref. 15, but we multiply all of them by a factor of  $f = 0.42$  since RPA overestimates the tendency towards magnetism.

We first show in Fig.1 the Fermi surface for various values of the doping rate  $x$ . The hole Fermi surfaces ( $\alpha_1$ ,  $\alpha_2$ ) around the wave vector  $(0,0)$  originating from the  $d_{XZ}/d_{YZ}$  orbitals shrink, while the electron Fermi surfaces ( $\beta_1$ ,  $\beta_2$ ) around  $(0,\pi)/(\pi,0)$  become larger with doping, as expected. What is interesting is that the volume of the hole Fermi surface ( $\gamma$ ) around  $(\pi,\pi)$ , which originates from the  $d_{X^2-Y^2}$  orbital, barely changes with doping for both materials. This is due to the band structure variation with doping, whose origin can be two folded. One is the lattice structure variation, and the other is the change in the electric charge of the FeAs and  $LnO$  layers. Both effects are taken into account in the present band calculation, and it turns out that the latter effect actually dominates. Namely, the energy level of  $d_{XZ}/d_{YZ}$  orbitals (that are oriented toward the  $LnO$  layers) is pushed down relative to  $d_{X^2-Y^2}$  owing to the increase of the positive charge in the  $LnO$  layers. Comparing the two materials, the  $\gamma$  Fermi surface is larger for Sm1111 due to higher pnictogen position.<sup>9)</sup>

In Fig.2, we show the Stoner factor as a function of  $x$ . It can be seen that the Stoner factor actually increases with doping for a fixed electron-electron interaction, as opposed to a naive expectation based on “rigid band + Fermi surface nesting” picture. To see this in more detail, we show in Fig.3 the ratio of the “intra-orbital spin susceptibility” between  $d_{X^2-Y^2}$  and  $d_{XZ}/d_{YZ}$  orbitals.<sup>9)</sup> Here, the intra-orbital spin susceptibility is defined as the diagonal element of the spin susceptibility matrix that has the same orbital indices. In La1111, the  $d_{XZ}/d_{YZ}$  susceptibility dominates for small doping, but as the doping rate is increased,  $d_{X^2-Y^2}$  tends to dominate, particularly around the wave vector  $(\pi, \pi/3)/(\pi/3, \pi)$ .<sup>16)</sup> The contribution to this wave vector comes from two interactions; one from the  $\gamma$ - $\beta$  (electron-hole, arrow 1 in Fig.1) interaction, and another from  $\beta_1$ - $\beta_2$  (electron-electron, arrow 2) interaction.<sup>9,17-19)</sup> These two contributions, both coming mainly from the intra-orbital re-

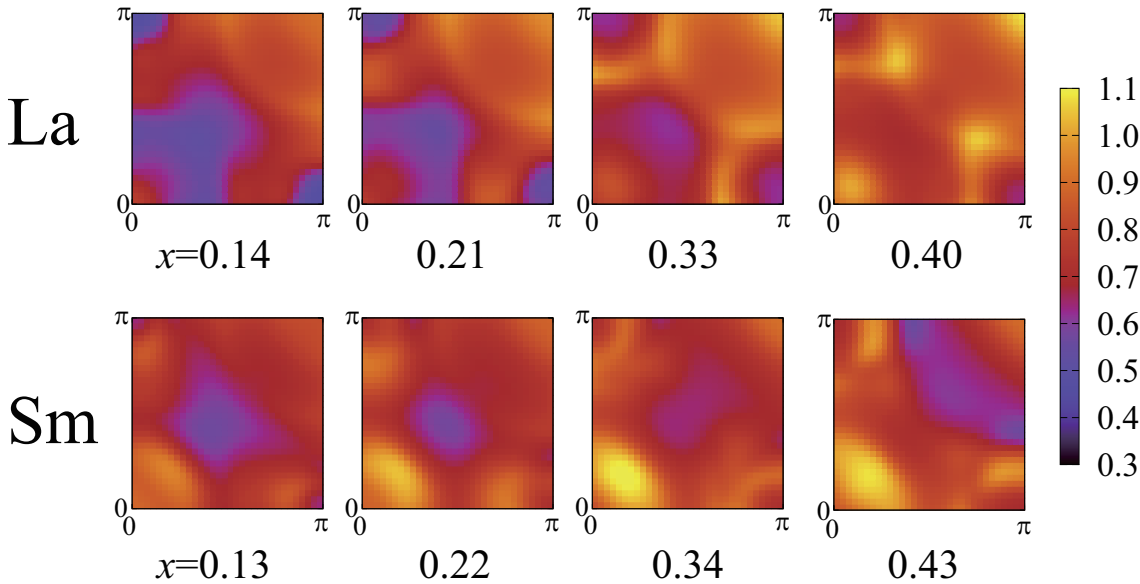


**Fig. 3.** (Color online) The ratio of the intra-orbital spin susceptibilities  $\chi_{X^2-Y^2}^s/\chi_{XZ/YZ}^s$  for various doping rate for La1111(top) and Sm1111(bottom).

pulsion within the  $d_{X^2-Y^2}$  orbitals, cooperate to give a large enhancement in the incommensurate spin fluctuations. In fact, the enhancement of the spin fluctuation around this wave vector is consistent with a recent experimental study.<sup>20)</sup> The cooperation occurs because the two contributions accidentally have similar incommensurate wave vectors especially for large  $x$  ( $\sim 0.3 - 0.4$ ). As for the material dependence, the difference between La1111 and Sm1111 can be seen by comparing the upper and lower panels in Fig3. While a crossover from  $d_{XZ}/d_{YZ}$  to  $d_{X^2-Y^2}$  dominating regimes is seen in La, the  $d_{X^2-Y^2}$  contribution is large through the entire doping regime for Sm1111. This is due to the presence of the larger  $\gamma$  Fermi surface in the latter material.

The two origins for the spin fluctuations, i.e., the  $\gamma$ - $\beta$  and  $\beta_1$ - $\beta_2$  interactions, cooperate toward antiferromagnetic instability, but they have competing effects regarding the occurrence of superconductivity. Namely, as discussed in previous studies,<sup>3,9,17-19)</sup> the  $\gamma$ - $\beta$  interaction leads to  $s\pm$  pairing, while the  $\beta_1$ - $\beta_2$  interaction favors  $d$ -wave pairing because this interaction acts to change the gap sign between  $\beta_1$  and  $\beta_2$ . To see which one of the interactions dominate in the pairing interaction, we calculate the eigenvalue of the Eliashberg equation for  $s$  and  $d$ -wave pairings. As shown in Fig.4(a),  $s$ -wave always dominates over  $d$ -wave, and the gap function has the fully gapped  $s\pm$  form as shown in Fig.4(b), where the gap changes sign between the electron and hole Fermi surfaces.

The present result suggests that the  $d_{X^2-Y^2}$  hole Fermi surface plays an important role in the occurrence of superconductivity even in the heavily doped regime. One should note, however, that the nesting (in the conventional sense of the term) between the electron and the hole Fermi surfaces is not good, since the volume is very different. Nevertheless, the pairing is strongly enhanced. This is because the portions of the bands away from the

Fermi level contribute to the pairing interaction through finite energy virtual processes. Therefore, one should be careful about using the word ‘‘Fermi surface nesting’’ as the origin of the pairing interaction, at least in the naive sense of the term.

The material dependence seen in the intra-orbital contribution to the spin susceptibility is also reflected to superconductivity. In Fig.4(c), we plot the eigenvalue of the Eliashberg equation against the doping rate for the two materials. We see that it is strongly enhanced in the heavily doped regime for La1111, while the variation is relatively weak for Sm1111. This is because the contribution weight to the spin fluctuations from the  $d_{X^2-Y^2}$  orbital is less dependent on the doping rate in Sm compared to that in La. The weak doping dependence of  $\lambda$  in Sm1111 is qualitatively consistent with the small variance of  $T_c$  for a wide range of  $x$  observed in Sm1111.<sup>6)</sup>

Here, we should comment on some discrepancies with the experimental observations. In both cases,  $\lambda$  monotonically increases with doping, and  $\lambda$  for La is larger than Sm. In the actual experiments,  $T_c$  has two (single) dome shape dependence against doping in La (Sm), and the maximum  $T_c$  is higher for Sm. Our present understanding is that this discrepancy comes from overestimating the effect of the density of states (DOS) variance in the RPA calculation. Namely, the band width decreases with doping and is also smaller in La than in Sm, which is directly reflected in the strength of the spin fluctuations and thus  $\lambda$ . In reality, the increase in DOS enhances the self energy correction (neglected in RPA), which suppresses the spin fluctuation and  $\lambda$ . Thus our expectation is that such a DOS variance overestimation effect is reduced in calculation that considers self energy corrections, which is now underway. Although a complete understanding of the shape of the phase diagram lies beyond the present theoretical approach, smaller eigenvalues obtained for small  $x$  in La1111 suggests a fragile

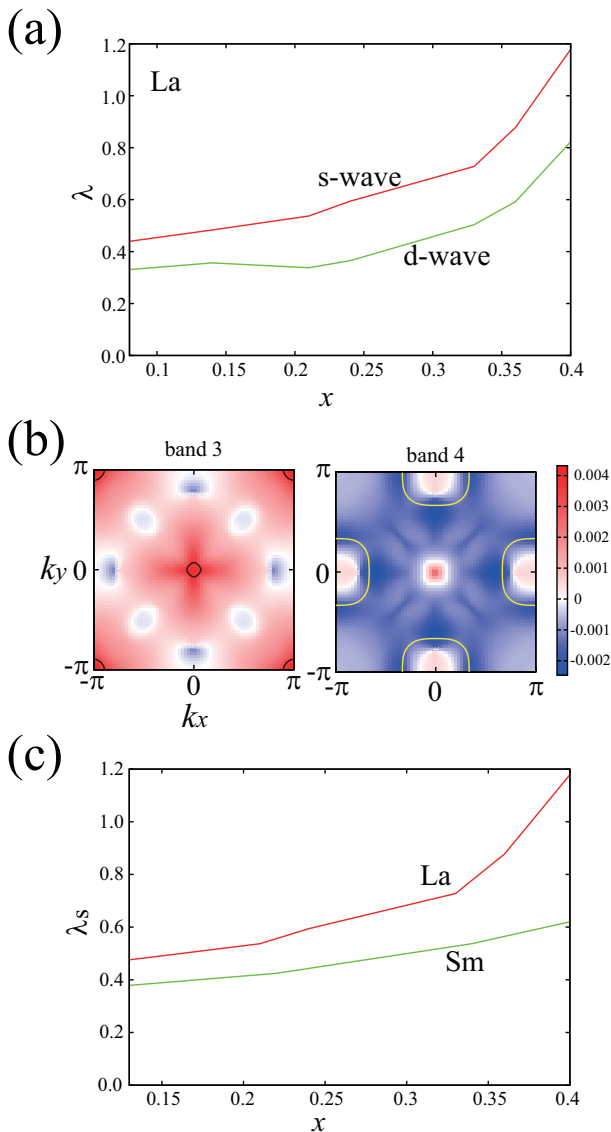


**Fig. 4.** (Color online) (a) The eigenvalue of the Eliashberg equation as a function of the doping for La1111. (b) The gap function for the  $s$ -wave pairing for band 3 (with the hole Fermi surfaces) and band 4 (the electron Fermi surfaces). The solid lines represent the Fermi surfaces. (c) The eigenvalue for the  $s$ -wave pairing against the doping rate for La and Sm.

nature of the superconductivity in this regime.

To summarize, we have analyzed the spin fluctuation and superconductivity of the 1111 iron pnictides in a wide range of electron doping rate by taking into account the band structure variation within the virtual crystal approximation. The  $d_{X^2-Y^2}$  hole Fermi surface around  $(\pi, \pi)$  is found to be robust for the entire doping regime, and plays an important role on both the spin fluctuations and superconductivity. In La1111, the  $d_{XZ}/d_{YZ}$  orbitals have relatively large contribution in the small  $x$  regime, while in Sm1111, the  $d_{X^2-Y^2}$  dominates over the entire regime. This difference in the  $d_{X^2-Y^2}$  contribution is plausibly the origin of the difference in the phase diagram between the two materials. After completion of this study, a paper that studies a similar problem for  $\text{LaFeAsO}_{1-x}\text{H}_x$  has been posted on the arXiv.<sup>21)</sup>

The numerical calculations were performed at the Su-

percomputer Center, ISSP, University of Tokyo. This study has been supported by Grant-in-Aid for Scientific Research No.24340079 from JSPS. K.S. acknowledges support from JSPS. The part of the research at Tokyo Institute of Technology was supported by the JSPS FIRST Program.

- 1) Y. Kamihara, T. Watanabe, M. Hirano, and H. Hosono: J. Am. Chem. Soc. **130** (2008) 3296.
- 2) I. I. Mazin, D. J. Singh, M. D. Johannes, and M. H. Du: Phys. Rev. Lett. **101** (2008) 057003.
- 3) K. Kuroki, S. Onari, R. Arita, H. Usui, Y. Tanaka, H. Kontani, and H. Aoki: Phys. Rev. Lett. **101** (2008) 087004.
- 4) For a review, see, e.g., K. Kuroki : Chapter 8 in *Iron-based superconductors*, ed. by N.-L.Wang, H. Hosono, and P. Dai, Pan Stanford Publishing, 2012.
- 5) S. Iimura, S. Matsuishi, H. Sato, T. Hanna, Y. Muraba, S. W. Kim, J. E. Kim, M. Takata, and H. Hosono: Nat. Commun. **3** (2012) 943 .
- 6) T. Hanna, Y. Muraba, S. Matsuishi, N. Igawa, K. Kodama, S. Shamoto, and H. Hosono: Phys. Rev. B **84** (2011) 024521.
- 7) H. Ikeda : J. Phys. Soc. Jpn. **77** (2008) 123707.
- 8) H. Ikeda, R. Arita, and J. Kuneš : Phys. Rev. B **81** (2010) 054502.
- 9) K. Kuroki, H. Usui, S. Onari, R. Arita, and H. Aoki: Phys. Rev. B **79** (2009) 224511.
- 10) T. Yamada and Y. Ōno : arXiv : 1209.4954.
- 11) G. Kresse and J. Hafner: Phys. Rev. B **47** (1993) 558; G. Kresse and J. Furthmüller: Phys. Rev. B **54** (1996) 11169 (<http://cms.mpi.univie.ac.at/vasp/vasp/vasp.html>) Here we adopt GGA-PBEsol exchange correlation functional introduced by John P. Perdew, Adrienn Ruzsinszky, Gábor I. Csonka, Oleg A. Vydrov, Gustavo E. Scuseria, Lucian A. Constantin, Xiaolan Zhou, and Kieron Burke: Phys. Rev. Lett. **100** (2008) 136406, and the wave functions are expanded by plane waves up to cut-off energy of 550eV.  $10^3$   $k$ -point meshes are used.
- 12) N. Marzari and D. Vanderbilt: Phys. Rev. B **56** (1997) 12847; I. Souza, N. Marzari, and D. Vanderbilt: Phys. Rev. B **65** (2001) 035109. The Wannier functions are generated by the code developed by A. A. Mostofi, J. R. Yates, N. Marzari, I. Souza, and D. Vanderbilt, (<http://www.wannier.org/>).
- 13) K. Yada and H. Kontani: J. Phys. Soc. Jpn. **74** (2005) 2161.
- 14) T. Takimoto, T. Hotta, and K. Ueda: Phys. Rev. B **69** (2004) 104504.
- 15) T. Miyake, K. Nakamura, R. Arita, and M. Imada: J. Phys. Soc. Jpn. **79** (2010) 044705.
- 16) There is also an “enhancement” of the  $\chi_{X^2-Y^2}^s$  vs.  $\chi_{XZ/YZ}^s$  ratio around the wave vector  $(0,0)$ , especially for Sm1111. Note, however, that this does not imply enhanced ferromagnetic fluctuations because it is the *ratio* that is enhanced, not the bare values. The bare values around  $(0,0)$  is small compared to those around  $(\pi,0) \sim (\pi,\pi/3)$ .
- 17) S. Graser, T. A. Maier, P. J. Hirschfeld, and D. J. Scalapino: New J. Phys. **11** (2009) 025016.
- 18) F. Wang, H. Zhai, and D.-H. Lee: Phys. Rev. B **81** (2010) 184512.
- 19) R. Thomale, C. Platt, W. Hanke and B.A. Bernevig: Phys. Rev. Lett. **106** (2011) 187003.
- 20) S. Iimura, S. Matsuishi, M. Miyakawa, T. Taniguchi, K. Suzuki, H. Usui, K. Kuroki, R. Kajimoto, M. Nakamura, K. Ikeuchi, S. Ji, and H. Hosono: submitted.
- 21) Y. Yamakawa, S. Onari, H. Kontani, N. Fujiwara, S. Iimura, and H. Hosono: arXiv: 1304.3933.